H_α and H_β, respectively. Values for the corresponding force constants in ethyl iodide of 0.535 and 0.647 mdyn Å/rad^2 have been reported by Durig et al.[41] On comparison of these force constants, a slight decrease is observed in the value of H_α for ethyl iodide whereas the value of H_β increases by 0.01 mdyn Å/rad^2. This trend is basically the same as the one observed for the analogous force constants of the silicon compounds, but the magnitude of the shift in the force constant values is not as great for the carbon compounds.

Conclusions

The microwave, infrared, and Raman spectra of disilyl iodide and disilyl-d_5 iodide have been recorded. The refined structural parameters obtained from the diagnostic least-squares analysis of the rotational constants are consistent with the corresponding parameters reported for other silyl and disilyl compounds. Of special interest is the value of 2.40 ± 0.009 Å obtained for the Si–I bond distance, which is statistically the same as the Si–I bond distance reported for silyl iodide. This agreement indicates that there is no detectable $p_\pi \rightarrow d_\pi$ back-bonding between the silicon and iodine atoms as suggested by the early NMR study.[7] If this proposed back-bonding existed, one would also anticipate a shortening of the Si–Si bond distance; no shortening in this bond distance was observed in disilyl iodide. As it turned out, the Si–Si bond distance was found to be the most invariant of all of the disilyl structural parameters during the least-squares adjustment process. The value of 2.336 Å obtained for this bond distance in disilyl iodide is very consistent with the Si–Si bond distance of 2.332 Å found in elemental silicon.[43] The results of the normal-coordinate analysis of disilyl iodide also yield considerable information about the Si–I bond. Comparison of the value of 1.57 mdyn/Å obtained for the Si–I stretching force constant of disilyl iodide to the value of 1.95 mdyn/Å reported for the corresponding bond in silyl iodide[34] suggests that the Si–I bond of disilyl iodide is weaker and has less single-bond character than the Si–I bond of silyl iodide. The force field obtained for disilyl iodide was in general very consistent with the force fields reported for several other silyl and disilyl compounds.[12] The major differences were found in the values reported for the SiH_3 and SiH_2 bending force constants. These differences, however, were found to follow the trend observed for the corresponding force constants of ethane[42] and ethyl iodide.[41] Considerable mixing was found between the SiH_3 and SiH_2 bending modes while the Si–H stretching modes and skeletal motions were found to be fairly pure. No information on the barrier to internal rotation of the SiH_3 group was obtained as the low vapor pressure and limited stability of the compound prevented the recording of Raman data for the gas phase with a good signal-to-noise ratio.

Acknowledgment. The authors gratefully acknowledge the financial support of this research by the National Science Foundation by Grant CHE-79-20763.

Registry No. H_3SiSiH_2I, 14380-76-8; D_3SiSiD_2I, 79568-43-7.

(43) *Spec. Publ.—Chem. Soc.*, No. 11 (1958).

Contribution from the Molecular Theory Laboratory, The Rockefeller University, Palo Alto, California 95304, IBM Research Laboratory, San Jose, California 95193, and Guelph-Waterloo Centre for Graduate Work in Chemistry, Department of Chemistry, University of Guelph, Guelph, Ontario, Canada N1G 2W1

Electronic Spectra and Structure of Bis(ethylene-1,2-dithiolato)nickel and Bis(propene-3-thione-1-thiolato)nickel

ZELEK S. HERMAN, ROBERT F. KIRCHNER, GILDA H. LOEW,* ULRICH T. MUELLER-WESTERHOFF,* ADEL NAZZAL, and MICHAEL C. ZERNER

Received January 28, 1981

The electronic ground states and spectra of $Ni(S_2C_2H_2)_2$ [bis(ethylene-1,2-dithiolato)Ni] and $Ni(S_2C_3H_3)_2$ [bis(propene-3-thione-1-thiolato)Ni] have been calculated with an INDO-type LCAO–MO CI program recently developed for treating systems containing transition-metal atoms. The ground-state descriptions obtained for these two compounds are consistent with the greater stability of $Ni(S_2C_2H_2)_2$ relative to $Ni(S_2C_3H_3)_2$ and also with the existence of mono- and dianions of the former. The electronic spectra of these compounds were assigned with utilization of extensive configuration interaction to describe the ground and excited states. The calculated transitions agree reasonably well with the energies and nature of the experimentally observed ones. In particular, low-energy transitions are found for $Ni(S_2C_2H_2)_2$, consistent with the observed spectra of $Ni(S_2C_2R_2)_2$-type compounds. These transitions are not found for $Ni(S_2C_3R_3)_2$, which is also in agreement with experiment.

Introduction

Square-planar complexes of Ni, Pd, and Pt with sulfur-containing conjugated ligands are interesting examples of complexes in which highly delocalized covalent bonding determines their observed properties.[1-4] Two characteristic types of such complexes are the bis(ethylene-1,2-dithiolato) complexes, $M(S_2C_2R_2)_2$ (I), and their bis(propene-3-thione-1-thiolato) analogues, $M(S_2C_3R_3)_2$ (II).

The parent compounds of type I with R = H are formed as a dianion from disodium salts of *cis*-dimercaptoethylene and the salts MCl_2, and two one-electron oxidations lead to the neutral species.[5-8] The exact nature of the bonding in these

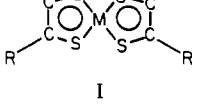

I

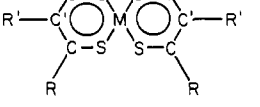

II

complexes has been somewhat uncertain. Several bonding pictures are possible for the neutral complexes (I), the most

* To whom correspondence should be addressed: G.H.L., The Rockefeller University; U.T.M.-W., IBM Research Laboratory.

(1) Schrauzer, G. N.; Mayweg, V. P. *J. Am. Chem. Soc.* **1961**, *84*, 3221.
(2) Schrauzer, G. N. *Transition Met. Chem.* **1968**, *4*, 299; *Acc. Chem. Res.* **1969**, *2*, 73.
(3) McCleverty, J. A. *Progr. Inorg. Chem.* **1968**, *10*, 49.
(4) Davison, A.; Edelstein, N.; Holm, R. H.; Maki, A. H. *J. Am. Chem. Soc.* **1963**, *10*, 2029.

0020-1669/82/1321-0046$01.25/0

likely of which are summarized as follows: 8 π-electron structures (not including the four metal d_π electrons)

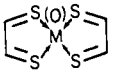

Ia

10 π-electron systems

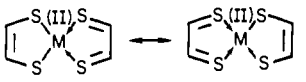

Ib

and 12 π-electron systems

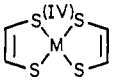

Ic

In the above, the arrows designate coordinate-covalent bonding. The M(IV) structure is possible, but less likely for M = Ni than for M = Pd or Pt. Proton magnetic resonance spectra and infrared C–S and C–C stretching frequencies strongly favor the equivalent delocalized aromatic structures (Ib).[5,9]

The neutral planar complexes (I), with M = Ni, Pt, or Pd, all have characteristic electronic spectra with an intense band at low energies. The energy of this band is sensitive to substituents, and it has been described as a $\pi \rightarrow \pi^*$ transition.[4] By proper choice of substituents, it has been possible[8] to shift this band as far as 1.4 μm. In this study, we shall examine the nature of this excitation, which is complicated by the presence of several possible valence-bond structures, all related by *two*-electron transfers, opposed to the usual one-electron excitations.

The parent compounds of type II can be prepared from tetraethoxypropane, HCl, H_2S, and the MX_2 halides.[10] In compounds of this type, the ligand anions contain six π electrons, and the neutral, ground-state species is, in turn, most likely represented by the bonding pictures IIa–c, although there exist, of course, many others.

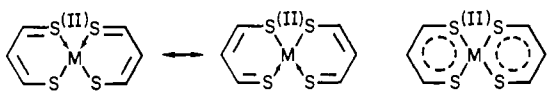

IIa IIb IIc

In the structures IIa and IIb, there are two covalent and two coordinate-covalent M–S bonds, and the metal is in a formal +2 oxidation state. Such compounds are considered less "aromatic" than type I compounds, but the average of IIa and IIb also yield a very delocalized bonding picture (IIc). Indeed, the ^1H NMR spectra of these compounds speak for a high degree of delocalization.[10] Recently, a semiquantitative evaluation has proven that type I *and* type II complexes show a high degree of cyclic electron delocalization.[11] Type II complexes do not have an intense near-infrared band in their electronic spectra in contrast to the strong, low-energy band observed for type I complexes.[10,12]

In the past, simple molecular orbital methods have been applied[6,12] to characterize both the bonding and the electronic spectra of type I and type II complexes of Ni, Pd, and Pt. While such investigations have been helpful in the assignment of the spectra, recent advances in methodology now make possible more accurate descriptions of both the structure and spectra of transition-metal complexes.

In the study reported here, we have utilized the intermediate neglect of differential overlap (INDO) method,[13-16] which includes configuration interaction (CI); this method is well suited for calculating the spectroscopic properties of transition-metal complexes.[15,16] Within this framework, we have calculated the electronic structure of the ground states of compounds I and II, with R = H and M = Ni, and assigned the electronic spectra of these compounds.

Noteworthy among the previous calculations on $Ni(Si_2C_2R_2)_2$ systems are the extended Hückel-type calculations of Schrauzer and Mayweg.[6] This investigation yielded results for the ground state in qualitative agreement with those reported here (although their Wolfsberg–Helmholtz parameters were chosen to yield results in accord with their intuition). In addition, the results of Schrauzer and Mayweg for the first few excited states are in remarkable agreement with ours, but there exist considerable discrepancies in the assignments for the higher energy states.

Similar extended Hückel-type calculations have been performed by Siimann and Fresco[12] on $Ni[C_3H(CH_3)_2S_2]_2$ [bis(dithioacetylacetonato)nickel(II)]. Their results for this type II compound with R′ = CH_3 and R = H are in qualitative agreement with ours for R′ = R = H.

Very recently, multiconfiguration self-consistent-field plus configuration interaction calculations on the dianion of $Ni(Si_2C_2H_2)_2$ have been published by Blomberg and Wahlgren.[17] Although not reported in depth here, we have also examined this ion to calibrate with their results: the ground-state description we obtain is very similar to that these authors reported. In addition, a prior brief summary of ab initio calculations on complexes of type I and related species with oxygen- and nitrogen-containing ligands has been published.[18] Where possible, comparison between these and our results is made in the present paper.

Methods and Procedure

The calculations were performed with a recently developed INDO–SCF–CI program which allows for the treatment of transition-metal complexes and the inclusion of extensive configuration interaction. This method, including the procedure for calculating electronic spectra, is summarized elsewhere.[13-16,19] Briefly, INDO/1, in which the one-center integrals are obtained from ionization potentials only, rather than from ionization potentials and electron affinities, is used to calculate the ground-state configuration in terms of molecular orbital coefficients and eigenvalues. A characteristic feature of this program is that it includes the evaluation of all one-center exchange terms necessary for rotational invariance. The program includes options for both theoretical and empirical evaluation of two-center repulsion integrals, the latter employing an empirical Weiss–Mataga–Nishimoto formula.[20,21]

(5) Schrauzer, G. N.; Mayweg, V. P. *J. Am. Chem. Soc.* **1965**, *87*, 3586.
(6) Cotton, F. A.; Wilkinson, G. "Advanced Inorganic Chemistry", 4th ed.; Interscience: New York, 1980, pp 185–187.
(7) Browall, K. W.; Interrante, L. V. *J. Coord. Chem.* **1973**, *3*, 27.
(8) Mueller-Westerhoff, U. T.; Nazzal, A.; Mayerle, J. J., to be submitted for publication.
(9) Schläpfer, C. W.; Nakamoto, K. *Inorg. Chem.* **1975**, *14*, 1338.
(10) Mueller-Westerhoff, U. T.; Alscher, A. *Angew. Chem., Int. Ed. Engl.* **1980**, *19*, 638.
(11) Nazzal, A.; Mueller-Westerhoff, U. T. *Transition Met. Chem.* **1980**, *5*, 318.
(12) Siimann, O.; Fresco, J. *J. Am. Chem. Soc.* **1970**, *92*, 2652.
(13) Ridley, J.; Zerner, M. *Theor. Chim. Acta* **1973**, *32*, 111.
(14) Ridley, J.; Zerner, M. *Theor. Chim. Acta* **1976**, *42*, 223.
(15) Bacon, A. D.; Zerner, M. C. *Theor. Chim. Acta* **1979**, *53*, 21.
(16) Zerner, M. C.; Loew, G. H.; Kirchner, R. F.; Mueller-Westerhoff, U. T. *J. Am. Chem. Soc.* **1980**, *102*, 589.
(17) Blomberg, M. R. A.; Wahlgren, U. *Chem. Phys.* **1980**, *49*, 117.
(18) (a) Fischer-Hjalmars, I.; Henriksson-Enflo, A. *Int. J. Quantum Chem.* **1980**, *18*, 409. (b) Demoulin, D.; Fischer-Hjalmars, I.; Henriksson-Enflo, A.; Pappas, J. A.; Sandbom, M. *Ibid.* **1977**, *12* (Suppl. 1), 351.
(19) Correa de Mello, P.; Hehenberger, M.; Larsson, S.; Zerner, M. C. *J. Am. Chem. Soc.* **1980**, *102*, 1278.

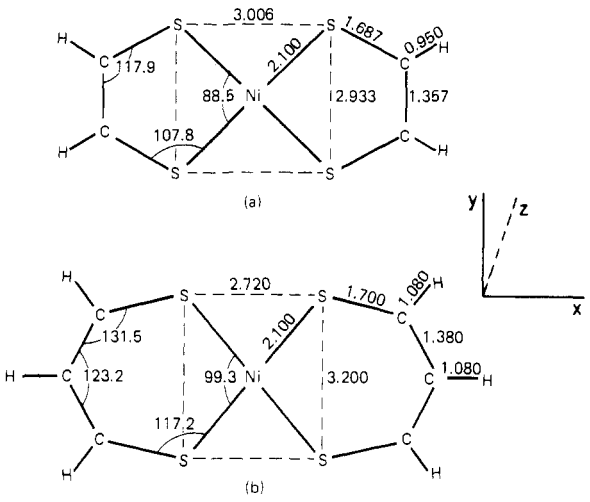

Figure 1. Regularized structures of (a) NiBDT and (b) NiPTT. Both molecules belong to point group D_{2h}. Distances are given in Å and angles in degrees. The C–H distances in NiBDT are unusually short but are based on structural data from ref 36. The NiPTT structure is extrapolated from the data for $Co(SacSac)_2$ in ref 28.

In order to guarantee convergence for systems containing transition metals and specific configurations, the program allows for specifying the occupancy of metal d orbitals and utilizes a "dynamic damping" procedure.[22] The empirical parameterization was designed for use with configuration interaction to calculate electronic transition energies. For the ground state, this spectroscopic parameterization partially restores Koopmans' theorem and appears to give reliable ionization potentials as well as one-electron properties such as the electric field gradient at the metal nucleus. We have recently tested this method in the assignment of the electronic and photoelectronic spectra of ferrocene[16] and in calculating the electric field gradient and spectral properties of model heme proteins.[23-27] In each case, excellent agreement with experiment was obtained.

The geometry of the $Ni(S_2C_2H_2)_2$ (NiBDT) complex was taken from a crystal structure determination[8] and regularized to give D_{2h} symmetry. The geometry of the $Ni(S_2C_3H_3)_2$ (NiPTT) complex was taken from a crystal structure of bis(dithioacetyleneacetonato)cobalt(II)[28] with D_{2h} symmetry and bond distances and angles estimated for the Ni(II) complex. The exact geometries used for each complex are given in Figure 1.

For both complexes, ground-state SCF calculations were made using the spectroscopic parameterization. For NiBDT, calculations were done for a number of values of the resonance parameter β_{3d} ranging from −32.0 to −20.0 eV. The best assignment of the spectra was found for $\beta_{3d}(Ni) = -25.0$ eV, but the results are not very sensitive to this variation, so that even a 20% change in the value of $\beta_{3d}(Ni)$ does not significantly alter them. The parameters for sulfur were chosen to give good agreement between the calculated and observed spectra of thioacetone and thiophene. All other parameters are as used in ref 13 and 16, except for $\beta_{3d}(Ni)$ just discussed. The relevant parameters are listed in Table I.

Table I. INDO/S Parameters

	H	C	S[a]	Ni[b]
$\zeta_s = \zeta_p(B.R.)^{-1}$	1.2	1.625	1.925	1.473
$\zeta_d(B.R.)^{-1}$			1.731	3.7765–2.3168
$\beta(s)$, eV	−12.0	−17.0	−14.0	−1.0
$\beta(d)$, eV			4.0	−25.0
$F^2(pp)$		4.55	4.57	2.42
$G^1(sp)$		6.95	3.10	1.06
$G^2(sd)$			3.25	0.84
$G^1(pd)$			4.31	0.37
$F^2(pd)$			3.45	0.75
$G^3(pd)$			2.57	0.40
$F^2(dd)$			3.55	9.90
$F^4(dd)$			2.31	6.60

[a] The Slater–Condon factors of sulfur come from atomic spectroscopy: $\beta(s)$ and $\beta(d)$ are from studies on thioacetone and thiophene and smoothing over these parameters for phosphorus, sulfur and chlorine. [b] Nickel parameters are from ref 15, except (3d) which is from this study; see text.

So that the spectrum of each compound could be assigned, the molecular orbitals of the ground states obtained by an SCF calculation were symmetry analyzed and assigned a representation in D_{2h} symmetry. A possible lowering of the ground-state energy by configuration interaction was also explored. With use of the symmetry analysis as a guide, a set of doubly excited configurations of appropriate symmetry was selected to interact. Since the INDO program currently can handle a maximum of 210 configurations, a strategy was adopted whereby an initial set of configurations thought to be important was selected for interaction. Those configurations which did not contribute significantly were eliminated and others were added until nearly the whole manifold of occupied orbitals and all the important virtual orbitals were explored. A final 210-dimensional CI calculation was then made for each of the eight irreducible representations with the most important excitations selected from all previous excited states explored in this iterative process. From the results of this set of eight final CI calculations, the electronic spectral transitions were assigned.

Transition moments and oscillator strengths were also calculated for each transition with use of the dipole length operator. The electronic spectra of $Ni(S_2C_2H_2)_2$ and $Ni(S_2C_3H_3)_2$ were assigned from the spectroscopic transition energies and oscillator strengths obtained by these CI calculations.

For the lowest energy state of $Ni(S_2C_2H_2)_2$ (I) and of $Ni(S_2C_3H_3)_2$ (II), the electronic structure, i.e., the nickel–ligand bonding and extent of delocalization, was investigated with a Mulliken population analysis of the SCF eigenvectors under the assumption that the INDO basis is a symmetrically orthogonalized Slater basis. The aim of this analysis was to determine and compare the Ni–S and ligand binding in the two complexes and determine the extent of their "aromaticity" and the formal valence state of Ni in these complexes.

From a theoretical point of view, there are several interesting features of a configuration interaction calculation which go beyond single excitations. Double excitations interact strongly with the reference wave function that is the principal component of the ground state and only with certain of the single excitations. Since a singles-only CI often presents a reasonable description of the spectrum of a given molecule, the inclusion of doubles most often destroys this agreement by lowering the ground state and only certain singles. The agreement, or "balance", is generally not restored until certain triply excited configurations—those that are double excited with respect to the low-lying single excitations—are included.[29] Since the

(20) Weiss, K., unpublished results.
(21) Mataga, M.; Nishimoto, K. *Z. Phys. Chem.* **1957**, *13*, 140.
(22) Zerner, M.; Hehenberger, M. *Chem. Phys. Lett.* **1979**, *52*, 550.
(23) Rohmer, M. M.; Loew, G. H. *Int. J. Quantum Chem., Quantum Biology Symp.* **1979**, *6*, 93.
(24) Herman, Z. S.; Loew, G. H. *J. Am. Chem. Soc.* **1980**, *102*, 1815.
(25) Loew, G. H.; Herman, Z. S.; Zerner, M. C. *Int. J. Quantum Chem.* **1980**, *19*, 481.
(26) Loew, G. H.; Rohmer, M. M. *J. Am. Chem. Soc.* **1980**, *102*, 3655.
(27) Loew, G. H.; Goldblum, A. *J. Am. Chem. Soc.* **1980**, *102*, 3657.
(28) Beckett, R.; Hoskins, B. F. *Chem. Comm.* **1967**, 909.
(29) See, for example: Hay, P. J.; Shavitt, I. *J. Chem. Phys.* **1974**, *66*, 2856.

size of the configuration interaction proceeds roughly as nm for single excitations, where n and m are the number of occupied and nonoccupied molecular orbitals considered in the excitations, as $n^2m^2/4$ for double excitations, and as $n^3m^3/36$ for triple excitations, this more "proper" treatment becomes a formidable task for even the simplest molecules, even within the zero-differential-overlap approximation employed here.

Very often the introduction of semiempirical two-electron integrals yields striking results even at the singles only CI level. In some cases, such as NiBDT, however, the presence of low-lying double excitations actually in the spectroscopic region of interest necessitates their explicit consideration; that is, semiempirical parameters might be expected to correct for higher lying excitations not explicitly included in the CI, but they cannot correct for excitations actually in the spectroscopic region of interest.[16,30,31] With the explicit consideration of low-lying double excitations, the role that the semiempirical two-electron repulsion integrals perform is somewhat uncertain. Without semiempirical parameters, we might expect poor results when compared to experiment because of the imbalance we have introduced in our treatment of ground and excited states. If we assume that the introduction of semiempirical parameters is to correct for higher *energy* excitations not explicitly considered, as opposed to double, triple, quadruple, etc., excitations, then this imbalance might be reduced or eliminated. There is some evidence for the latter interpretation from many-body perturbation theory calculations over localized bonds.[32,33] In these cases the perturbation theory appears to converge much more rapidly when employing semiempirical integrals than when employing theoretically calculated integrals, suggesting use of the former is self-correcting.

Our study on NiBDT and NiPTT using single excitations, and single and double excitations, further adds to our information on this question. The inclusion of doubles in the examination of NiPTT does not greatly influence our results from a singles only treatment of this molecule, a result typical of most molecules. For NiBDT our results are somewhat affected by the inclusion of double excitations, leading to results in better agreement with experiment for the lower lying states than a "singles-only" calculation. The higher energy states with larger transition strengths are reasonably well represented by our "singles-only" calculation, better perhaps than they are with our "singles and doubles" calculation. Preliminary studies with triples, however, indicate that these higher energy states are still affected. This is as might be expected: the higher energy states lie close in energy to the triples and higher excitations and mix to a greater extent than do the lower lying states which are "further" away. Tentatively, we believe that the inclusion of higher excitations—and in particular triple excitations—will improve the results we have obtained using semiempirical parameters but will not have the severe effect expected on an ab initio singles and doubles treatment, where their inclusion is often essential. There is a growing amount of evidence, however, that a theory including singles, doubles, and triples might require a reparameterization of the pure parameter, β, and perhaps, reexamination of the functional form of the Coulomb integral used.

In addition to the above considerations, one might question the role of sulfur 3d orbitals on the calculated spectra of such compounds as NiBDT and NiPTT. Since the bonding in the ground state of these compounds is not unusual, their inclusion should not have a great effect on ground-state properties. As the sulfur 3d orbitals represent low-lying excited states for the atom, however, they might contribute to the spectrum of the compounds investigated. We report calculations on NiBDT and NiPTT both with and without sulfur 3d orbitals. As will be seen, the inclusion of sulfur 3d orbitals affects the calculated energies of the higher lying states only slightly, but, more important for the classification of the spectrum, they affect the predicted oscillator strengths of these excitations, especially in the case of NiBDT.

Results and Discussion

(A) Electronic Structure. The $Ni(S_2C_2H_2)_2$ complex (NiBDT) has 54 valence electrons. The energy and character of the orbitals calculated from an INDO/1-type SCF procedure with spectroscopic parameterization is given in Table II, together with the seven lowest empty orbitals. In the D_{2h} molecular symmetry, the d_{z^2} and $d_{x^2-y^2}$ orbitals belong to a_g, d_{xy} to b_{1g}, d_{xz} to b_{2g}, and d_{yz} to b_{3g} representations. Ligand π orbitals are of a_u, b_{1u}, b_{2g}, and b_{3g} type, while ligand σ orbitals belong to a_g, b_{1g}, b_{2u}, and b_{3u} representations. As seen in Table II, the first 10 orbitals and orbitals 12, 13, 21, and 25, i.e., 14 orbitals, are nearly pure ligand σ orbitals, the latter two corresponding to nonbonding sulfur orbitals. By contrast, only three filled orbitals, 16, 23, and the highest occupied orbital, 27 (HOMO), are nearly pure ligand π orbitals. The remaining 10 filled orbitals all have some Ni as well as ligand character. These orbitals are heavily mixed; that is, it is difficult to categorize these orbitals as either ligand or metal d orbitals. There are four a_g orbitals with d_{z^2} and $d_{x^2-y^2}$ character, numbers 11, 15, 20, and 22. Two of these are ligand σ orbitals with forward donation to d_{z^2} and $d_{x^2-y^2}$ orbitals and two are formally $d_{z^2} \pm d_{x^2-y^2}$ orbitals, but all are highly mixed with substantial d and ligand σ character. The b_{1g} orbital (d_{xy}), which is the formally empty orbital number 29 in this Ni(II) d^8 diamagnetic singlet ground state, acquires electron density by forward donation from ligand bonding orbitals b_{1g} MOs 10, 17, and 19. The π molecular orbitals are also delocalized, the $1b_{2g}$ ligand bonding orbitals (number 14) has significant (21%) d_{xz} character, and the $2b_{3g}$ bonding orbital (number 26) has significant (28%) d_{yz} character. The corresponding filled d antibonding orbitals $2b_{2g}$ (number 24) and $1b_{3g}$ (number 18) have significant ligand character and are 64% d_{xz} and 72% d_{yz}, respectively. The lowest empty molecular orbital ($3b_{2g}$, LEMO) is also a ligand π orbital with significant (16%) d_{xz} character. We note that the orbital energy of this orbital is quite negative, (−0.15 au), even more negative than the LEMO energy of −0.11 au resulting from an ab initio calculation[18] on NiBDT. It can be inferred from Koopmans' theorem, which equates the negative of this orbital eigenvalue with the molecule's electron affinity, that negative ions of $Ni(S_2C_2H_2)_2$ should be stable. Uninegative and dinegative ions are known experimentally.[4,5]

The inclusion of the sulfur 3d orbitals into the calculation does not greatly alter the results of the SCF ground state. The orbital eigenvalues, reported in Table II in parentheses, of the occupied orbitals are generally lowered by 0.01 a.u. or less. The virtual orbitals are somewhat more affected as expected. There are some reversals in ordering, but these are confined to close lying molecular orbitals. With the inclusion of 3d atomic orbitals on sulfur, for example, the $8a_g$ unoccupied MO is pushed up above the $2a_u$ level, representing the greatest change. Most of the occupied MOs have less than 1% sulfur 3d character. The few exceptions are reported in the table. Again, as expected, the unoccupied orbitals acquire greater sulfur 3d character.

Extensive configuration interaction with the SCF ground state was performed. These studies imply that the reference configuration of Table I accounts for 87% of the ground-state description. About 4% of the ground state is calculated as $2b_{1u}^2 \rightarrow 3b_{2g}^2$ ($HOMO^2 \rightarrow LEMO^2$), which suggests the delocalized

(30) Iwato, S.; Freed, K. *J. Chem. Phys.* **1974**, *61*, 1500; *Chem. Phys. Lett.* **1974**, *28*, 176.
(31) Brardow, B. H. *Int. J. Quantum Chem.* **1979**, *15*, 207.
(32) Malrieu, J. P.; Claveire, P.; Diner, S. *Theoret. Chim. Acta* **1969**, *13*, 18.
(33) Cullen, J.; Zerner, M. C., unpublished data.

Table II. Nature and Energy of Molecular Orbitals in $Ni(S_2C_2H_2)$ (Orbitals 1-27 Occupied)

MO	orbital energy,[a] au		sym[b]	type	% S 3d[c]
1	−1.40	(−1.41)	$1b_{3u}$	L_σ	
2	−1.39	(−1.40)	$1a_g$	L_σ	
3	−1.02	(−1.02)	$1b_{2u}$	L_σ	
4	−1.00	(−1.01)	$1b_{1g}$	L_σ	
5	−0.95	(−0.95)	$2a_g$	L_σ + 0.21 Ni s	
6	−0.93	(−0.94)	$2b_{3u}$	L_σ − 0.21 Ni p_x	
7	−0.77	(−0.77)	$2b_{2u}$	L_σ + 0.23 Ni p_y	
8	−0.71	(−0.72)	$3a_g$	L_σ	
9	−0.69	(−0.70)	$3b_{3u}$	L_σ	
10	−0.69	(−0.69)	$2b_{1g}$	L_σ + 0.19 d_{xy}	
11	−0.64	(−0.64)	$4a_g$	L_σ − 0.17 d_{z^2} − 0.20 $d_{x^2-y^2}$ + 0.19 Ni s	
12	−0.53	(−0.53)	$3b_{2u}$	L_σ	
13	−0.52	(−0.53)	$4b_{3u}$	L_σ	
14	−0.48	(−0.49)	$1b_{2g}$	L_π (±0.33 S p_z ± 0.29 C p_x) + 0.46 d_{xz}	
15	−0.48	(−0.48)	$5a_g$	L_σ (±0.10 S p_x ± 0.21 S p_y) + 0.45 d_{z^2} − 0.69 $d_{x^2-y^2}$	
16	−0.48	(−0.49)	$1b_{1u}$	L_π (0.36 S p_z + 0.34 C p_z)	
17	−0.47	(−0.48)	$3b_{1g}$	L_σ (±0.33 S p_x ± 0.23 C p_x) − 0.46 d_{xy}	1%
18	−0.45	(−0.46)	$1b_{3g}$	L_π (±0.26 S p_z) − 0.85 d_{yz}	
19	−0.43	(−0.43)	$4b_{1g}$	L_σ (±0.12 S s ± 0.39 S p_y ± 0.13 C p_x) + 0.47 d_{xy}	
20	−0.42	(−0.43)	$6a_g$	L_σ (±0.20 S p_y ± 0.12 C p_y) − 0.53 d_{z^2} − 0.67 $d_{x^2-y^2}$	1%
21	−0.40	(−0.40)	$5b_{3u}$	S_σ (−0.22 S p_x ± 0.38 S p_y ± 0.21 C p_y) + 0.27 Ni p_x	
22	−0.39	(−0.39)	$7a_g$	L_σ (±0.11 S p_x ± 0.28 S p_y ± 0.10 C p_y) + 0.66 d_{z^2} − 0.10 $d_{x^2-y^2}$	
23	−0.38	(−0.38)	$1a_u$	S_π (±0.49 S p_z ± 0.11 C p_z)	
24	−0.37	(−0.39)	$2b_{2g}$	L_π (±0.30 C p_z) − 0.80 d_{xz}	2%
25	−0.36	(−0.36)	$4b_{2u}$	S_σ (±0.14 S p_x − 0.44 S p_y) + 0.27 Ni p_y	
26	−0.36	(−0.36)	$2b_{3g}$	L_π (±0.41 S p_z ± 0.10 C p_z) − 0.53 d_{yz}	
27	−0.29	(−0.30)	$2b_{1u}$	L_π (0.34 S p_z − 0.36 C p_z)	2%
28	−0.15	(−0.15)	$3b_{2g}$	L_π*(±0.37 S p_z ± 0.27 C p_z) − 0.40 d_{xz}	1%
29	−0.01	(+0.03)	$5b_{1g}$	L_σ*(±0.10 S p_x + 0.28 S p_y) − 0.72 d_{xy}	4%
30	+0.04	(+0.03)	$8a_g$	L_σ*(0.10 S s ± 0.18 S p_x ± 0.28 S p_y) + 0.21 d_{z^2} − 0.84 Ni s	
31	+0.04	(+0.02)	$3b_{3g}$	L_π*(0.11 S p_z ± 0.49 C p_z)	6%
32	+0.04	(+0.02)	$2a_u$	L_π*(±0.11 S p_z ± 0.49 C p_z)	7%
33	+0.09	(+0.08	$5b_{2u}$	L_σ − 0.26 Ni p_y	7%
34	+0.10	(+0.09)	$3b_{1u}$	0.98 Ni p_z	2%

[a] First column, results of calculation without sulfur 3d AOs; in parentheses (second column), from calculation including 3d AOs on sulfur. [b] Numbering of orbitals of each symmetry type neglects core electron orbitals. So that absolute numbering of core orbitals can be obtained, add: 8 to a_g, 5 to b_{1g}, 1 to b_{2g}, 1 to b_{3g}, 1 to a_u, 3 to b_{1u}, 7 to b_{2u}, and 7 to b_{3u}. [c] The percentages of S(3d) character are not given for molecular orbitals with less than 1%.

description of structure Ib. The remaining 9% of the ground state is scattered over many configurations, none of which accounts for more than 2% and most of which are metal-to-ligand charge transfer.

Table III lists the molecular orbital energies and character for the odd π-electron ligand complex $Ni(S_2C_3H_3)_2$ (NiPTT), which contains 64 electrons. The extent of orbital delocalization is even greater in this complex than in NiBDT. There are eight occupied π-type MOs, containing 16 "π electrons", 12 of which are associated with ligands, in accord with our anticipated structure II.

Figure 2 shows the correlation of the MOs for the two complexes. The salient feature of this diagram is that the HOMO of NiPTT correlates with the LEMO of NiBDT. Furthermore, the HOMO of NiBDT is ligand π orbital while the two lowest virtual orbitals of NiPTT are ligand π orbitals. As seen in this figure, the predominantly Ni3d MOs in NiBDT and NiPTT all have about the same percentage metal character.

In contrast to the case for NiBDT, the lowest empty orbital in NiPTT virtually has no Ni 3d character. Moreover, the orbital energy of this orbital is not nearly as negative as that for the LEMO in NiBDT (−0.05 vs. −0.15 au). Therefore, we do not expect the negative ions of $Ni(S_2C_3H_3)_2$ to be as stable as those of $Ni(nS_2C_2H_2)_2$.

This correlation is also consistent with the observed electrochemical behavior of NiBDT and NiPTT complexes.[34] Complexes of the NiBDT type undergo up to four electrochemical reductions.[2-5,35] The first two of these electrons are thought to add to a predominantly ligand-based orbital of b_{2g} symmetry, in keeping with the calculated LEMO. Subsequent reductions lead to the formation of rare d^9 and d^{10} complexes and are thought to involve a metal-based b_{1g} orbital, again consistent with the availability of such an orbital among the next higher empty orbitals. For NiPTT complexes, however, the electrons added by corresponding reductions have all been assigned[34] to predominantly ligand orbitals, based on the significant observed sensitivity of the first and second reduction potentials to ligand variation. This result is again consistent with those presented in Figure 2 and at odds with the calculated MOs of Siimann and Fresco.[12]

In examining this question somewhat further, we have performed SCF and SCF–CI calculations on the dinegative ion of NiBDT. The two additional electrons have been added to the $3b_{2g}$ orbital as suggested by Table II. The orbital energy of this occupied level is now 0.11 eV (compared with 1.2 eV from ref 17 and 1.9 eV from ref 18), a value indicating stability for a dinegative ion. The dinegative ion is predicted from these ΔSCF calculations to be more stable than the neutral species only by 0.15 au, a value in good agreement with the Koopman's sum of $\epsilon^0(3b_{2g}) + \epsilon^{-2}(3b_{2g}) = -0.15$ au, which assumes that the relaxation energy of the dinegative ion loosing electrons, and of the neutral species gaining electrons, cancel. Configuration interaction calculations indicate that the ground

(34) Bowden, W. L.; Holloway, J. D. L.; Geiger, W. E., Jr. *Inorg. Chem.* **1978**, *17*, 256.
(35) Senftleber, F. C.; Geiger, W. E., Jr. *J. Am. Chem. Soc.* **1975**, *97*, 5018.
(36) Results obtained by A. E. Smith, communicated to us by J. S. Kasper and L. V. Interrante.
(37) Mayerle, J. J. *Inorg. Chem.* **1976**, *16*, 916.
(38) Kaufman, J. J. *Int. J. Quantum Chem.* **1971**, *4*, 205.

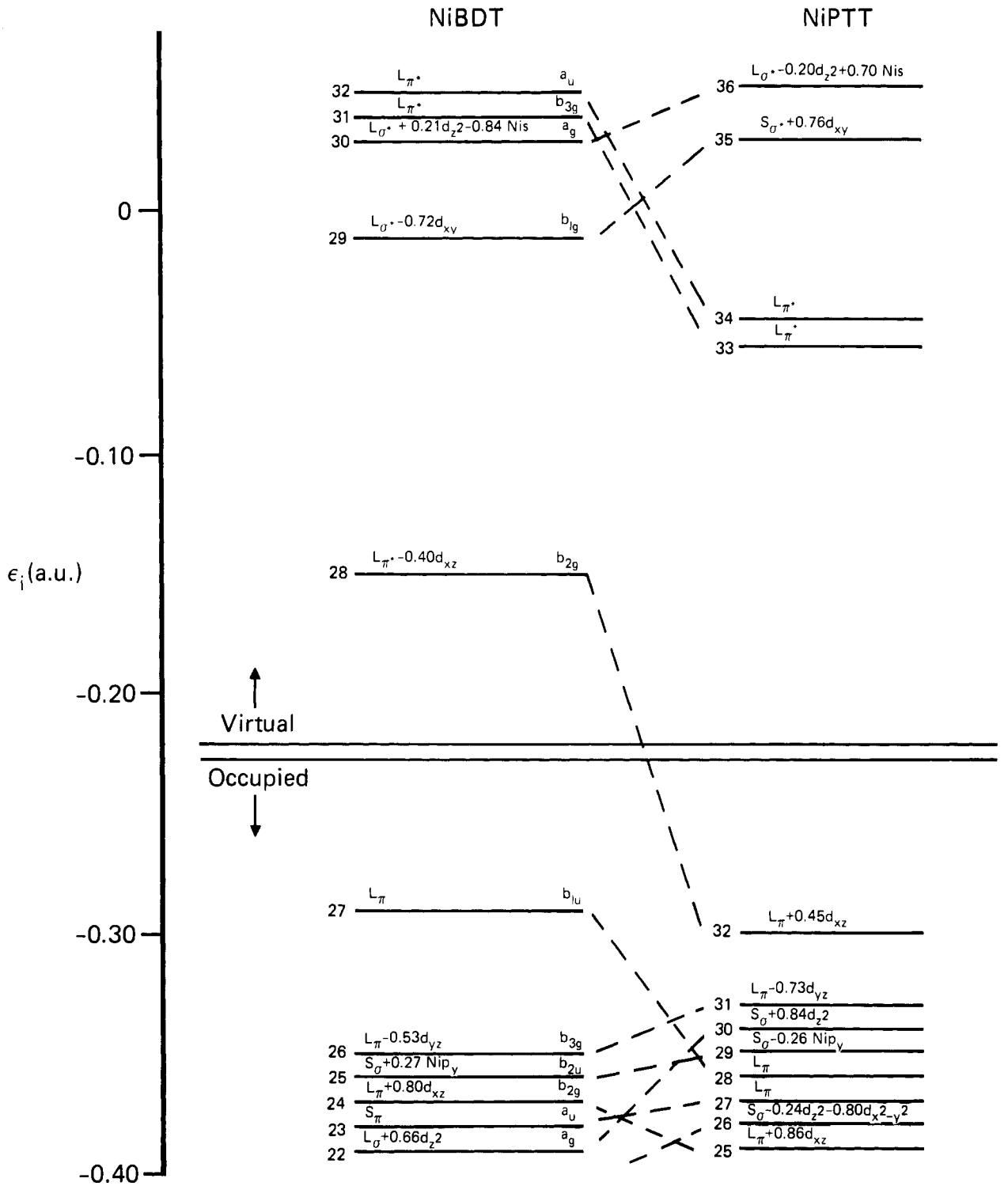

Figure 2. Correlation of MOs of NiBDT and NiPTT. Observe that the HOMO of NiPTT correlates with the LEMO of NiBDT.

states of NiBDT and $(NiBDT)^{2-}$ are lowered by about the same value, 1.78 eV. This value is considerably larger than the value of 0.64 eV reported by Blomberg and Wahlgren[17] from their MC-SCF-CI calculations on $(NiBDT)^{2-}$.

Extensive CI calculations on the ground state of $Ni(S_2C_3H_3)_2$ were also performed. In contrast to the situation for NiBDT, the reference configuration of Table III accounts for 95% of the ground state description. The principal CI component of the ground state is not ($HOMO^2 \rightarrow LEMO^2$) but rather $5b_{1g}^2$(number 24) $\rightarrow$ $6b_{1g}^2$(number 35), with a contribution of only 1% of the SCF-CI ground state.

A Mulliken population analysis of the filled MOs of NiBDT and NiPTT yields the electronic structures summarized in Table IV. The net charge on the Ni and the d orbital population corresponds closely to a Ni(II) d^8 configuration in both complexes. Net charges of +1.86 and +1.80, respectively, on the Ni atoms are similar in both complexes and small net deviations from +2 are the result of extensive forward and back-donation as described above, as are deviations from two electrons in each filled d orbital. The formally empty d_{xy} orbitals have 1.01 and 0.77 electrons each due to coordinate-covalent bonding. The sulfur atoms in NiBDT each have a -0.59 charge in keeping with the totally delocalized description of NiBDT combining equivalent structures Ib. The net charge on the carbon atoms in NiBDT is nearly 0, with the H atoms acquiring a positive charge. In our opinion, the

Table III. Nature and Energy of Molecular Orbitals in $Ni(S_2C_3H_3)_2$ (Orbitals 1-32 Occupied)

MO	orbital energy,[a] au		sym[b]	type	% S 3d[c]
1	−1.42	(−1.43)	$1b_{3u}$	L_σ	
2	−1.42	(−1.42)	$1a_g$	L_σ	
3	−1.13	(−1.13)	$1b_{2u}$	L_σ	
4	−1.12	(−1.12)	$1b_{1g}$	L_σ	
5	−1.00	(−1.00)	$2a_g$	L_σ + 0.18 Ni s	
6	−0.98	(−0.99)	$2b_{3u}$	L_σ − 0.16 Ni p_x	
7	−0.86	(−0.86)	$2b_{2u}$	L_σ + 0.20 Ni p_y	
8	−0.80	(−0.80)	$2b_{1g}$	L_σ	
9	−0.79	(−0.80)	$3a_g$	L_σ	
10	−0.79	(−0.80)	$3b_{3u}$	L_σ	
11	−0.75	(−0.75)	$4a_g$	L_σ − 0.10 d_{z^2} − 0.14 $d_{x^2-y^2}$	
12	−0.66	(−0.66)	$3b_{2u}$	L_σ	
13	−0.63	(−0.64)	$4b_{3u}$	L_σ	
14	−0.55	(−0.55)	$3b_{1g}$	L_σ − 0.20 d_{xy}	
15	−0.54	(−0.55)	$5a_g$	L_σ − 0.29 $d_{x^2-y^2}$	
16	−0.53	(−0.53)	$4b_{2u}$	L_σ	
17	−0.48	(−0.49)	$1b_{1u}$	L_π (0.26 S p_z − 0.23 C p_z − 0.39 C′ p_z)	
18	−0.48	(−0.49)	$1b_{2g}$	L_π (−0.24 S p_z − 0.31 C p_z ± 0.39 C′ p_z) − 0.24 d_{xz}	1%
19	−0.46	(−0.48)	$4b_{1g}$	L_σ + 0.27 d_{xy}	1%
20	−0.44	(−0.44)	$6a_g$	L_σ + 0.39 d_{z^2} − 0.50 $d_{x^2-y^2}$	
21	−0.43	(−0.44)	$5b_{3u}$	L_σ	
22	−0.43	(−0.43)	$1b_{3g}$	L_π (±0.35 S p_z ± 0.13 C p_z) − 0.67 d_{yz}	
23	−0.39	(−0.39)	$6b_{3u}$	S_σ (0.19 S p_x ± 0.42 S p_y) − 0.29 Ni p_x	
24	−0.38	(−0.40)	$5b_{1g}$	S_σ (±0.40 S p_y) + 0.51 d_{xy}	2%
25	−0.38	(−0.40)	$2b_{2g}$	L_π (±0.15 S p_z ± 0.13 C p_z ± 0.23 C′ p_z) + 0.86 d_{xz}	1%
26	−0.38	(−0.40)	$7a_g$	S_σ (0.21 S p_y) − 0.24 d_{z^2} − 0.80 $d_{x^2-y^2}$	2%
27	−0.38	(−0.38)	$1a_u$	L_π (0.46 S p_z + 0.20 C p_z)	
28	−0.35	(−0.35)	$2b_{1u}$	L_π (0.41 S p_z − 0.14 C p_z − 0.34 C′ p_z)	
29	−0.35	(−0.35)	$5b_{2u}$	S_σ (0.45 S p_y) − 0.26 Ni p_y	
30	−0.34	(−0.35)	$8a_g$	S_σ (±0.18 S p_y) + 0.84 d_{z^2} + 0.38 Ni s	
31	−0.33	(−0.34)	$2b_{3g}$	L_π (±0.39 S p_z ± 0.16 C p_z) − 0.73 d_{yz}	1%
32	−0.30	(−0.31)	$3b_{2g}$	L_π (±0.40 S p_z ± 0.25 C′ p_z) + 0.45 d_{xz}	
33	−0.05	(−0.06)	$3b_{3g}$	L_π* (±0.19 S p_z ± 0.46 C p_z)	3%
34	−0.05	(−0.06)	$2a_u$	L_π* (±0.20 S p_z ± 0.46 C p_z)	3%
35	+0.03	(+0.01)	$6b_{1g}$	S_σ* (±0.11 S s ± 0.28 S p_y) + 0.76 d_{xy}	4%
36	+0.06	(+0.05)	$9a_g$	L_σ* (−0.15 S s ± 0.19 S p_y − 0.15 C s − 0.12 C′ s) − 0.20 d_{z^2} + 0.70 Ni s	2%
37	+0.07	(+0.07)	$3b_{1u}$	L_π* (−0.36 C p_z + 0.48 C′ p_z)	3%
38	+0.07	(+0.06)	$4b_{2g}$	L_π* (±0.36 C p_z ± 0.48 C′ p_z)	4%
39	+0.08	(+0.07)	$6b_{2u}$	L_σ* + 0.24 Ni p_y	6%
40	+0.09	(+0.08)	$10a_g$	L_σ* + 0.48 Ni s	1%
41	+0.09	(+0.09)	$7b_{3u}$	L_σ*	2%
42	+0.13	(+0.12)	$4b_{1u}$	0.98 Ni p_z	3%

[a] First column, results of calculation without sulfur 3d-AOs; in parentheses (second column), from calculation including 3d AOs on sulfur. [b] Numbering of orbitals of each symmetry type neglects core electron orbitals. So that absolute numbering of orbitals can be obtained, add: 9 to a_g, 5 to b_{1g}, 1 to b_{2g}, 1 to b_{3g}, 1 to a_u, 3 to b_{1u}, 7 to b_{2u} and 8 to b_{3u}. [c] The percentages of S(3d) character are not given for molecular orbitals with less than 1%.

charge of 1.86 for Ni in NiBDT found in our calculation is more reasonable than the −0.07 charge derived from the ab initio calculation in ref 18. This latter value is rather unusual and indicates either a very odd bonding situation for the complex which our INDO calculations have not been able to pick up, or that the ab initio calculation has converged to a different state than the INDO calculation, or that there is a basis set imbalance favoring the metal population in the ab initio calculation. Nevertheless, since the present investigation provides a good description of the electronic spectrum of NiBDT (vide infra), the INDO results probably provide a proper representation of the ground state.

The inclusion of 3d orbital on sulfur in NiBDT has the rather unexpected effect of lowering the net negative charge on sulfur, from −0.59 to −0.48, in spite of the fact that the five 3d orbitals have picked up 0.05 electrons. Another interesting observation is that each neighboring carbon atom has become considerably more negative although the sum of the carbon and sulfur charges remain much the same. Both of these effects may be artifacts of the Mulliken population procedure which assigns charge to atoms according to overlap. The sulfur 3d atomic orbitals used are quite large (average radius about 1.4Å) and the shared region between carbon orbitals and sulfur 3d orbitals contributes 0.08 electrons to both carbon and sulfur atoms. If it is more reasonable to assign all of this charge to sulfur, then the net charges after the addition of sulfur 3d orbitals are much the same as before their addition. The inclusion of 3d orbitals on sulfur for NiPTT has much the same effect on the Mulliken population as their inclusion had in NiBDT, and a similar argument can be made.

The similarities in the electron distributions between NiBDT and NiPTT are more striking than their differences. From the results summarized in Table IV, there seems to be no obvious basis for considering NiBDT to be more "aromatic" than NiPTT although it does have somewhat more participation of the d_{yz} orbital in ligand bonding.

In Table IV, the experimental ^1H NMR chemical shifts, relative to Me_4Si are shown for each complex. They are consistent with the calculated proton charges.

(B) Electronic Spectrum of $Ni(S_2C_2H_2)_2$ (NiBDT). The experimental electronic spectrum of NiBDT in methanol solution has been presented by Schrauzer and Mayweg.[5] We found, however, that NiBDT slowly reacts with methanol and that the reported spectral data have to be revised. In particular, the first intense absorption at 13 900 cm^{-1} was reported to have a shoulder at 11 600 cm^{-1}. This shoulder belongs to a product of the reaction of NiBDT with the solvent. Allowing a fresh solution of NiBDT in methanol, which shows ϵ 14 900 cm^{-1} and no shoulder at 11 600 cm^{-1}, to stand overnight gives rise to a spectrum corresponding to the published one: the

Table IV. Net Atomic Charges and Atomic Orbital and Bond Overlap Densities in Two Ni(II) Square-Planar Complexes[a]

	$Ni(S_2C_2H_2)_2$	$Ni(S_2C_3H_3)_2$
	Net Atomic Charge	
q_{Ni}	+1.86 (+1.90)	+1.80 (+1.86)
q_S	−0.59 (−0.48)	−0.66 (−0.55)
q_C	0.00 (−0.12)	+0.10 (−0.04)
$q_{C'}$		−0.05 (−0.03)
q_H	+0.12 (+0.13) (9.25 ppm)[b]	+0.10 (+0.10) (8.73 ppm)[b]
$q_{H'}$		+0.07 (+0.07) (7.40 ppm)[b]
	Bond Overlap Densities[c]	
ρ(Ni-S)	0.54	0.52
ρ(S-C)	0.69	0.69
ρ(C-C)	1.01	0.96
ρ(S-S)	0.01	0.02
ρ(S-S')	0.01	0.01
ρ_π(Ni-S)	0.04	0.00
ρ_π(S-C)	0.07	0.08
ρ_π(C-C)	0.21	0.17
	Atomic Orbital Electron Population[d] for Ni	
4s	0.14 (0.15)	0.17 (0.17)
$4p_x$	−0.25 (−0.30)	−0.18 (−0.20)
$4p_y$	−0.21 (−0.25)	−0.37 (−0.43)
$4p_z$	0.02 (0.01)	−0.00 (−0.00)
d_{z^2}	1.90 (1.88)	1.86 (1.84)
$d_{x^2-y^2}$	1.99 (1.97)	1.99 (1.96)
d_{xy}	1.01 (1.08)	0.77 (0.87)
d_{xz}	1.55 (1.56)	2.00 (1.99)
d_{yz}	2.00 (1.98)	1.97 (1.94)
	Atomic Orbital Electron Population[a] for S	
s	2.16 (2.18)	2.15 (2.18)
p_x	1.24 (1.19)	1.07 (1.04)
p_y	1.50 (1.48)	1.64 (1.61)
p_z	1.68 (1.66)	1.80 (1.78)
d (all)	(0.05)	(0.01)
	Atomic Orbital Electron Population for C[e]	
s	1.33 (1.38)	1.35 (1.42) [1.23 (1.23)]
p_x	0.87 (0.89)	0.94 (0.95) [0.86 (0.87)]
p_y	0.90 (0.92)	0.95 (0.97) [0.85 (0.86)]
p_z	0.93 (0.94)	0.66 (0.70) [1.10 (1.07)]

[a] Numbers in parentheses correspond to values obtained in the calculation with sulfur 3d orbitals. [b] Observed NMR chemical shift in $CDCl_3$ solution, relative to Me_4Si. [c] Bond overlap density ρ(A-B) defined by

$$\rho(AB) = \sum_k^{MO} \sum_{ij}^{AO} c_{iA}{}^k c_{jB}{}^k S_{ij} \quad \text{(ref 38)}$$

[d] Mulliken populations with the assumption that the INDO basis corresponds to a symmetrically orthogonalized set of STO's. [e] Numbers in square brackets represent values for C'.

13 900-cm^{-1} absorption has lost half its intensity and a strong shoulder at 11 600 cm^{-1} has appeared. The shape of the intense band at 13 900 cm^{-1} of even a fresh solution of NiBDT in methanol is such that the presence of a very weak (ϵ <400) shoulder could be postulated, if one would want to insist on it. The high-energy portion of the published spectrum needs to be corrected as well. We found that the peak at 34 500 cm^{-1} has ϵ 26 360 with a shoulder at 37 000 cm^{-1} and that the last absorption below 50 000 cm^{-1} occurs at 47 600 cm^{-1} (ϵ 19 900), instead of at 42 590 cm^{-1} (ϵ 4,400). Near 42 000 cm^{-1}, there exists a very distinct minimum.

The experimental spectrum for fresh solutions in methanol is identical with that of a solution in hexane, in which solvent the NiBDT complex appears to be much more stable. This spectrum is reproduced in Figure 3. The characteristic features are the very intense peak at 13 900 cm^{-1}, two weak, broad bands with maxima at 18 180 (shoulder at 22 500 cm^{-1}) and 27 000 cm^{-1}, and two intense bands with maxima at 34 480 and 47 620 cm^{-1}. The 34 480-cm^{-1} absorption has a shoulder

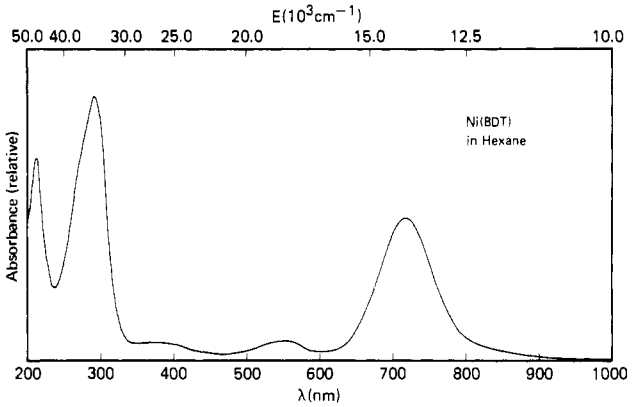

Figure 3. Absorption spectrum of NiBDT in hexane.

Table V. Main Features of the Experimental Electronic Spectra for NiBDT in Hexane and NiPTT in Methanol[a]

NiBDT			NiPTT	
position, cm^{-1}	intens[b] ϵ	intens[b] f	position, cm^{-1}	intens[c] (ϵ)
11 630	<400		13 790	225
13 900	14 300	0.10	17 390	2300
18 180	2300	~0.02	24 390	shoulder
22 500	shoulder		29 850	21 400
27 000	1850, br	0.05	35 210	shoulder
34 480	26 360		38 170	51 170
		0.82		
37 000	shoulder		42 190	shoulder
47 620	19 900	0.48	48 850	19 600

[a] See also Figures 2 and 3. [b] Experimental oscillator strength from Figure 2. [c] Extensive band overlap in the spectrum of NiPTT makes the determination of experimental oscillator strengths ambiguous. Only extinction coefficients are given.

at approximately 37 000 cm^{-1}. These values are compared to the spectrum of NiPTT in Table V.

In order to characterize this spectrum, we have utilized configuration interaction on the INDO/1 ground state of NiBDT. The configuration interaction consisted of all single excitations and extensive sets of single and double excitations symmetry factored for each of the eight irreducible representations belonging to the point group D_{2h}. In D_{2h} symmetry, only transitions to $b_{1u}(z)$, $b_{2u}(y)$, and $b_{3u}(x)$ states are allowed. Extensive CI involving all possible double excitations of appropriate symmetry lowered the ground state singlet (^1A_g) by 14 400 cm^{-1}. A summary of the transition energies relative to the SCF–CI ground state for NiBDT is listed in Table VI. Table VI includes all states calculated below 20 000 cm^{-1} but only the allowed ones above this value. There are many allowed transitions in the entire region of observed spectral transitions for NiBDT. These include L → L*, L → M*, and M → L* transitions of both σ and π types. In addition, there are numerous forbidden d → d* transitions which could be hidden under these allowed transitions. In contrast to previous assignments of the spectrum, none of the formally forbidden transitions need to be invoked to assign the strong observed transitions though they may be adding the intensity and shape of these bonds.

Most of the allowed transitions involve excitation to the LEMO $3b_{2g}$ (L_{π^*}) orbital. All transitions could be assigned principally to go to this orbital with smaller contributions from the $5b_{1g}$ (d_{σ^*}), $8a_g$ (L_{σ^*}), and $3b_{3g}$ (L_{π^*}) orbitals.

The strong band observed at 13 870 cm^{-1} is characteristic of neutral square-planar complexes of Ni, Pd, and Pt with $(S_2C_2R_2)_2$ ligands and is assigned $^1B_{3u}$. This excitation is principally HOMO → LEMO, ligand $\pi \rightarrow \pi^*$. From Table II it is seen that the nature of these molecular orbitals suggests

Table VI. Comparison of Calculated and Observed Spectra of NiBDT (Transition Energies in 1000 cm^{-1})

singles		singles, doubles with S(3d)	
no S(3d) $E(f)^b$	with S(3d) $E(f)^b$	$E(f)^b$ [% doubles]	obsd $E(f)$
	All States		
B_{2g} 6.9	B_{2g} 7.4	B_{2g} 10.1 [14]	
B_{1g} 7.3	B_{1g} 8.1		
A_u 10.5	A_u 9.5	B_{1g} 12.4 [12]	11.6 (wk)
B_{3u} 11.6 (0.47)	B_{3u} 11.6 (0.35)	B_{3u} 14.0 (0.13) [31]	13.9 (0.10)
B_{2g} 14.9	B_{2g} 16.4		
A_g 19.0			
B_{1u} 19.9 (0.001)	B_{1u} 19.0 (0.002)	B_{2u} 16.1 (0.03) [83]	18.2 (0.02)
	A_g 19.9	B_{1u} 16.3 (0.001) [98]	br
		A_u 16.8 [14]	
		A_g 18.5 [51]	
		B_{2g} 19.1 [15]	
	Allowed Only[a]		
		B_{1u} 23.5 (0.000) [88]	22.5 (sh)
B_{2u} 22.4 (0.19)	B_{2u} 21.3 (0.18)	B_{2u} 23.8 (0.12) [43]	27.0 (0.05)
		B_{2u} 24.8 (0.005) [99]	
		B_{1u} 25.4 (0.001) [77]	
		B_{1u} 26.9 (0.001) [55]	
		B_{3u} 28.2 (0.004) [94]	
		B_{2u} 28.7 (0.001) [99]	
		B_{1u} 29.4 (0.000) [97]	
B_{1u} 39.3 (0.01)	B_{1u} 37.5 (0.02)		
B_{3u} 42.2 (0.62)	B_{3u} 41.5 (0.83)	~36.0 (f_{calcd})	34.5 (0.82)
B_{1u} 43.0 (0.00)	B_{2u} 44.3 (0.08)		
B_{2u} 43.8 (0.01)	B_{2u} 44.7 (0.00)		
	B_{1u} 46.0 (0.08)		
	B_{1u} 46.1 (0.14)		
B_{3u} 45.5 (0.11)			
B_{1u} 46.1 (0.07)	B_{3u} 47.5 (0.43)	~45.0 ($1.5 - f_{calcd}$)	47.6 (0.48)
B_{2u} 46.7 (0.10)			
B_{3u} 47.1 (0.06)	B_{3u} 49.8 (0.52)		
B_{3u} 50.3 (0.74)			

[a] In the singles and doubles calculation there are 30 allowed states between 33 000 and 50 000 cm^{-1} and 48 forbidden. The exact intensity distribution among the heavily mixed allowed states is sensitive to higher excitations, although peaks at about 36 000 and 45 000 cm^{-1} seem stable with total oscillator strength of about 1.5; see text. These values are shown in the table. Ninety percent of this intensity is predicted to come from $^1B_{3u}$ states. [b] Oscillator strengths are not listed for symmetry-forbidden transitions.

that this transition should be quite sensitive to ligand variation and relatively insensitive to the transition element involved. This result is consistent with the unpublished results obtained in this laboratory[8] and of Schrauzer's observation[2] that this intense band, which is characteristic of all neutral and monoanionic dithienes of Ni, Pd, and Pt, is substituent dependent and hence must be $\pi \rightarrow \pi^*$.

Although the band observed with a maximum at 13 870 cm^{-1} is well represented in all these calculations of Table VI, and is characterized as principally HOMO → LEMO, the inclusion of double excitations affects the calculated intensity very strongly. The reason for this is that the ground state mixes with $(HOMO)^2 \rightarrow (LEMO)^2$, drastically reducing the intensity of the calculated excitation and yielding an oscillator strength in much better accord with experimental results. The very weak lower energy transition at 11 600 cm^{-1} is probably associated with a reaction product, as previously discussed, but, as Table VI shows, several transitions of $^1B_{2g}$ and $^1B_{1g}$ symmetry can be found in this region. Interesting is the removal, with the inclusion of doubles, of the A_u state from this region to higher energy. These low-lying states of $^1B_{2g}$ and $^1B_{1g}$ symmetry are principally $d_\pi \rightarrow L_{\pi^*}$ charge-transfer excitations. Although a careful study of the triplet states of NiBDT has not been made, preliminary studies indicate the triplet HOMO–LEMO excitation ($^3B_{3u}$) is also in this region, below 10 000 cm^{-1}.

The band observed at 18 180 cm^{-1} is broad and diffuse. The "singles-only" calculation associates this band principally with $^1B_{1u}$; the calculation with doubles suggests a more complicated assignment with most of the intensity coming from $^1B_{2u}$ which is found with 83% doubles character. As in the "singles-only" calculation, there is a weaker $^1B_{1u}$ state calculated in this region, but is nature has changed to be 98% doubles and is calculated to have very little oscillator strength ($f = 2.0 \times 10^{-4}$).

There is a broad transition with a maximum at about 27 000 cm^{-1} and a clear shoulder at 22 500 cm^{-1}. All these calculations associate most of the intensity of this peak with $^1B_{2u}$. The breadth of this peak, and the shoulder, could easily be explained by the great wealth of other transitions predicted in this region, both allowed (in the case of the singles and doubles excitations) and forbidden, not shown in the table, but characteristic of all three calculations.

Above 30 000 cm^{-1} all three calculations predict a high density of transitions, both allowed and forbidden. The allowed transitions are reported for both singles calculations, that is, with and without the inclusion of S_{3d} orbitals. In the singles and double calculation there is nearly a continuum of allowed states above 33 000 cm^{-1}, and although their calculated energy seems stable with respect to additional doubles and preliminary inclusion of triples, the intensity distribution among these states fluctuates strongly. The total oscillator strength calculated in this region, however, seems nearly constant at 1.34 for x, 0.13 for y, and 0.02 for z, the relative order consistent with dimensions of the molecule, and the total of 1.5 in reasonable accord with an experimental estimate of 1.4. The singles-only calculation without 3d sulfur orbitals does not have enough calculated intensities in this region, a very unusual occurrence for a theory which consistently overestimates intensity in all regions by a factor of about 2.

The inclusion of sulfur 3d orbitals, as seen from the table, gives results in much better accord with experiment. All

Table VII. Comparison of Calculated and Experimental Spectra of NiPTT (Transition Energies in 1000 cm^{-1})

singles				singles, doubles with no S(3d)		
no S(3d) $E(f)^b$		with S(3d) $E(f)^b$		$E(f)^b$ [% doubles]		obsd[a] E (ϵ)
			All States			
$^3B_{1g}$	15.6	$^3B_{1g}$	13.2			13.8 (225)
B_{3g}	19.4	B_{3g}	18.6	B_{3g}	18.8 [2]	17.4 (2300)
B_{1g}	19.8	B_{1g}	19.0	B_{1g}	19.4 [4]	
B_{2g}	21.3	B_{2g}	19.4	B_{2g}	19.5 [4]	
B_{1g}	23.7	B_{1g}	21.6	B_{1g}	22.0 [4]	
B_{2u}	24.3 (0.25)	B_{1g}	25.4	B_{2u}	24.2 (0.05) [19]	24.4 (sh, 2690)
B_{1g}	24.4	B_{2u}	26.1 (0.25)	B_{1g}	26.8 [9]	
B_{1u}	27.9 (0.01)	B_{1u}	29.9 (0.01)	B_{1u}	31.2 (0.04) [14]	
B_{2g}	28.0	B_{2g}	29.9			
B_{3g}	28.6	B_{3g}	30.0			
A_u	29.6	A_u	30.6			
			Allowed Only			
B_{3u}	32.3 (0.38)	B_{3u}	32.6 (0.27)	B_{3u}	31.6 (0.10) [14]	29.8 (21 400)
B_{2u}	36.2 (0.17)	B_{2u}	37.7 (0.24)			35.2 (sh, 17 400)
B_{3u}	41.0 (0.71)	B_{3u}	43.4 (0.60)			38.2 (51 700)
B_{2u}	43.6 (0.01)	B_{2u}	45.2 (0.01)			42.2 (15 250)
B_{1u}	44.7 (0.00)	B_{1u}	45.8 (0.00)			
B_{3u}	47.3 (0.11)	B_{3u}	50.4 (0.15)			48.8 (19 600)
B_{1u}	48.5 (0.03)	B_{1u}	51.7 (0.02)			

[a] Because of ambiguities in deriving experimental oscillator strengths from Figure 3, due to band overlap, the molar extinction coefficient is given for comparison. [b] Oscillator strengths are not listed for symmetry-forbidden transitions.

calculations suggest that the broad peak with a maximum at 34 500 cm^{-1}, and the sharper peak at 47 600 cm^{-1} are complex, and both owe most of their intensity to states of $^1B_{3u}$ symmetry. The intensities for these states calculated from the "singles and doubles" treatment are nearly random among some 30 states, although intensity maxima appear at about 36 000 and 45 000 cm^{-1}. It is possible that extensive CI of singles, doubles, and triples presently beyond our capabilities (or desires!) would be required before the intensities if these states "settled" down. The "singles-only" calculations with the 3d orbitals on sulfur present a reasonable and stable description of the spectrum in the region between 30 000 and 50 000 cm^{-1}, although the more intense peak calculated at 41 500 cm^{-1} is in rather poor numerical agreement with the experimentally observed peak at 34 500 cm^{-1}.

(C) Electronic Spectrum of $Ni(S_2C_3H_3)_2$ (NiPTT). The electronic spectrum of NiPTT is shown in Figure 4. As noted previously, the intense near-infrared peak that is characteristic of the NiBDT spectrum is absent here. There is a weak absorption at 17 390 cm^{-1}, with a very weak shoulder at 13 800 cm^{-1}, a broad, intense band in the region 20 500–33 300 cm^{-1} with a maximum at 29 850 cm^{-1}, and an intense band centered at 38 170 cm^{-1}. Finally, a broad peak begins around 45 000 cm^{-1}, with a maximum at 48 850 cm^{-1}.

Extensive configuration interaction on symmetry-adapted subsets of single and double excitations was performed as described previously for the eight irreducible representations belonging to the point group D_{2h}. The ground-state single (^1A_g) was lowered by 5900 cm^{-1}. The transition energies relative to the SCF–CI ground state for each symmetry type are listed in Table VII. In constrast to the situation for NiBDT, double excitations do not play a major role in the description of most of the observed transitions.

As can be seen from the Table VII, the agreement between the calculated and experimentally observed transitions is remarkably good. The weak transition at 17 390 cm^{-1} is assigned to a combination of forbidden transitions from the ground state to $^1B_{3g}$, $^1B_{1g}$, and $^1B_{2g}$ states. Although covalency between metal and ligand masks somewhat the nature of these states, they are mostly $b_{2g}(d_{xz}) \rightarrow b_{1g}(d_{xy})$, $a_g(d_{z^2}) \rightarrow b_{1g}(d_{xy})$, and $b_{3g}(d_{yz}) \rightarrow b_{1g}(d_{xy})$, respectively. The shoulder appearing at 24 390 cm^{-1} is assigned to the $^1B_{2u}$ state calculated at 24 200 cm^{-1}, corresponding to the transition $L_\pi \rightarrow L_{\pi^*}$. The forbidden transition to the $^1B_{1g}$ state, calculated at 22 000 cm^{-1}, may also contribute to this shoulder.

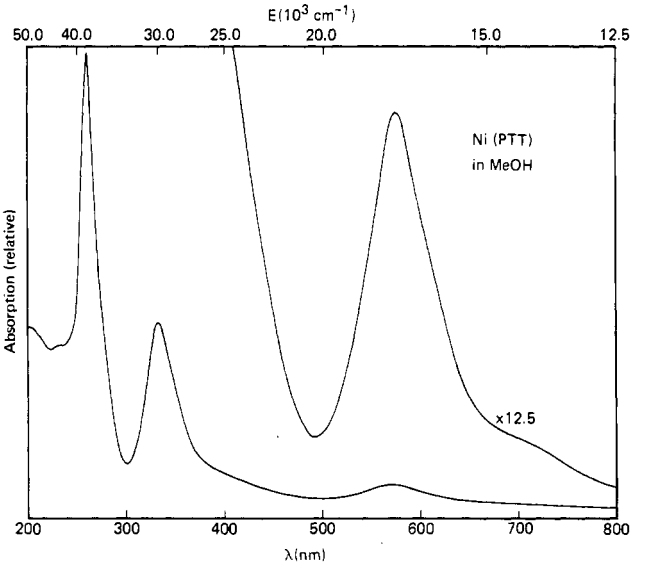

Figure 4. Absorption spectrum of NiPTT in methanol.

The first strong electronic adsorption in the NiPTT spectrum appears at 29 850 cm^{-1}, and this is assigned $^1B_{3u}$, although many forbidden states are also calculated in this region. This $^1B_{3u}$ is principally $d_{3g}(d_{yz}) \rightarrow a_u(L_{\pi^*})$, metal to ligand charge transfer which has gained intensity through the covalency of the b_{3g} orbital. Much of this intensity is removed by including double excitations, the result of which can be associated with the restoration of metal character to the b_{3g} orbital.

The shoulder appearing at 35 210 cm^{-1} is assigned $^1B_{2u}$ as shown in Table VII. This transition is mostly $b_{1u}(L_\pi) \rightarrow b_{3g}(L_{\pi^*})$.

The strong absorption at 38 170 cm^{-1} is assigned $^1B_{3u}$, although the many calculated forbidden states in this region may be contributing to the shape and intensity of this band. The $^1B_{3u}$ transition calculated at 41 000 cm^{-1} (without S(3d)) or 43 400 cm^{-1} (with S(3d)) is 65% $a_u(L_\pi) \rightarrow b_{3g}(L_{\pi^*})$, 18% $b_{2u}(L_\sigma) \rightarrow b_{1g}(d_{xy})$ and 12% $b_{3g}(L_\pi) \rightarrow a_u(L_{\pi^*})$. Although this band contains M → L* and L → M* charge-transfer com-

ponents, the CI indicates that they are balanced, with very little net charge-transfer resulting.

The peak observed at 48 850 cm^{-1} is assigned as $^1B_{3u}$. The shoulder at 42 190 cm^{-1} is assigned $^1B_{2u}$, although there is a $^1B_{1u}$ also calculated in this region at slightly higher energy, but before the onset of the more intense $^1B_{3u}$ transition. It is interesting that the $^1B_{3u}$ associated with most of the intensity in this region is calculated to have charge-transfer character consisting of 70% $b_{2u}(L_\sigma) \rightarrow b_{1g}(d_{xy})$ and 25% $a_u(L_\pi) \rightarrow b_{3g}(L_{\pi^*})$. Finally, the very weak shoulder found at 13 800 cm^{-1} may be associated with the lowest energy $^3B_{1g}$ calculated to be at about 13 200 cm^{-1}. This transition is calculated to be nearly pure $8a_g(d_{z^2}) \rightarrow 6b_{1g}(d_{xy})$.

Conclusions

The results of applying the newly developed INDO program to investigate the SCF-level ground states of $Ni(S_2C_2H_2)_2$ and $Ni(S_2C_3H_3)_2$ indicate that these two compounds have very similar electronic structures insofar as atomic charge, bond overlap density, and atomic orbital electron population are concerned. In both cases the nickel atom is in a formal oxidation state of +2 with a d^8 configuration. The principal valence-bond structure for $Ni(C_2S_2H_2)_2$ is the ten π-electron structure Ib although, according to the CI results, this structure provides only 87% of the ground-state description. Not surprisingly, structure II accurately describes the bonding in $Ni(S_2C_3H_3)_2$.

The differences in the energy and character of the two lowest empty orbitals of these compounds correspond to the experimentally observed differences in reduction behavior of the compounds and stability in their respective anions.

The major difference between these complexes is in the ordering of the highest filled and lowest empty molecular orbitals. These differences are reflected in the spectra and electron-accepting and -donating properties of the two compounds. On one hand, the highest occupied molecular orbital (L_π,d_π) of $Ni(S_2C_3H_3)_2$ corresponds to the lowest empty molecular orbital of $Ni(S_2C_2H_2)_2$. On the other hand, the LEMO of $Ni(S_2C_3H_3)_2$, a L_{π^*} orbital, corresponds to a higher energy virtual orbital of $Ni(S_2C_2H_2)_2$ while the HOMO (L_π) of $Ni(S_2C_2H_2)_2$ corresponds to a low-lying occupied orbital of $Ni(S_2C_3H_3)_2$.

Extensive configuration-interaction calculations, within the confines of the INDO/1 approximation, for the transitions between the ground and excited states yield good agreement with the experimentally observed electronic spectra of both compounds. In particular, the strong, near-infrared band, which is characteristic of $Ni(S_2C_2R_2)_2$ complexes, is well reproduced and is assigned to a transition between the ground state and the lowest $^1B_{1u}$ state, which is principally HOMO $\rightarrow$ LEMO $[b_{1u}(L_\pi) \rightarrow b_{2g}(L_\pi,d_\pi)]$ in character. The absence of such intense, low-lying transition in the case of $Ni(S_2C_3H_3)_2$ is a striking feature which is reproduced by our calculations and is due to the fact that *both* corresponding orbitals of b_{1u} and b_{2g} symmetry for this complex are doubly occupied.

We have examined the role of sulfur 3d orbitals in the calculation of ground- and excited-state properties of NiBDT and NiPTT. As might be anticipated by the rather normal bonding to sulfur in these complexes, the inclusion of sulfur 3d orbitals has very little influence on the ground-state calculation, nor are calculated transition energies, especially of the lower-lying states, much affected. The major influence of including these orbitals appears in adding transition strength to the region between 30 000–50 000 cm^{-1}, leading to much better agreement with experiment.

The presence of so many possible valence-bond structures in these compounds has prompted an examination utilizing both single and double excitations. The inclusion of double excitations has a much larger effect on the ground and low-lying excited states of NiBDT than on those of NiPTT. An extensive examination of the former was made with utilization of singles and doubles. The resulting calculated spectrum is in very good agreement with experiment, especially for the lower lying states where the calculated intensities are much improved. Above 33 000 cm^{-1} there is nearly a continuum of calculated states, both allowed and forbidden. Although there appear intensity peaks at about 36 000 and 45 000 cm^{-1}, in reasonably good agreement with experiment, the detailed assignment of intensities for states, especially among the $^1B_{3u}$ and $^1B_{2u}$ states is sensitive to further refinements of the calculation as discussed, making one-to-one correspondence between the observed and calculated transitions impossible.

Acknowledgment. This work was supported in part by grants from the National Research and Engineering Council of Canada and by National Science Foundation Grant PCM 76-07324. A special computer grant at the University of Guelph is gratefully acknowledged. We are very grateful to Dr. W. E. Rudge of the IBM Research Laboratory computer center for patient guidance in programming problems.

Registry No. NiBDT, 19042-52-5; NiPTT, 64705-83-5.